ORGANOMETALLICS

Article

Cite This: *Organometallics* XXXX, XXX, XXX−XXX

Development of a Novel Ferrocenyl Histone Deacetylase Inhibitor for Triple-Negative Breast Cancer Therapy

Chu Tang,[†,‡,#] Yang Du,[‡,§,∥,#] Qian Liang,[‡] Zhen Cheng,[*,⊥] and Jie Tian[*,†,‡,§,∥]

[†]Engineering Research Center of Molecular and Neuro Imaging, Ministry of Education, School of Life Science and Technology, Xidian University, Xi'an, Shaanxi 710126, People's Republic of China

[‡]CAS Key Laboratory of Molecular Imaging, The State Key Laboratory of Management and Control for Complex Systems, Institute of Automation, Chinese Academy of Sciences, Beijing 100190, People's Republic of China

[§]Beijing Key Laboratory of Molecular Imaging, Beijing 100190, People's Republic of China

[∥]University of Chinese Academy of Sciences, Beijing 100080, People's Republic of China

[⊥]Molecular Imaging Program at Stanford (MIPS), Department of Radiology, and Bio-X Program, Canary Center at Stanford for Cancer Early Detection, Stanford University, Stanford, California 94305-5344, United States

Supporting Information

ABSTRACT: Owing to the lack of target-directed therapies, triple-negative breast cancer (TNBC) is difficult to effectively treat. In this article, a novel organometallic histone deacetylase (HDAC) inhibitor, Fc-SelSA, based on the selenocyanide (SelSA) zinc-binding motif, was synthesized using a ferrocenyl group as the cap to confer activity against TNBC. The synthesized Fc-SelSA was evaluated for bioactivity in vitro and in vivo. An enzymatic assay showed that Fc-SelSA was a potent HDAC inhibitor with a half-maximum inhibitory concentration (IC_{50}) of 14.8 nM. Molecular docking studies of Fc-SelSA with HDAC suggested that the ferrocenyl unit overlaps with the phenyl group of suberoylanilide hydroxamic acid (SAHA) and the amido group of Fc-SelSA can form hydrogen bonds with the D98 and G151 residues of HDAC, but SAHA and SelSA do not show similar interactions. Moreover, Fc-SelSA reactivated the estrogen receptor alpha (ERα) expression, sensitized TNBC cells to the antagonist tamoxifen, and exerted more potent antitumor effects against TNBC MDA-MB-231 tumor xenografts in comparison to SelSA with no obvious side effects. Our results indicate that Fc-SelSA is a potent oral anticancer candidate for HDAC-targeted TNBC therapy and deserves further investigation for clinical application.

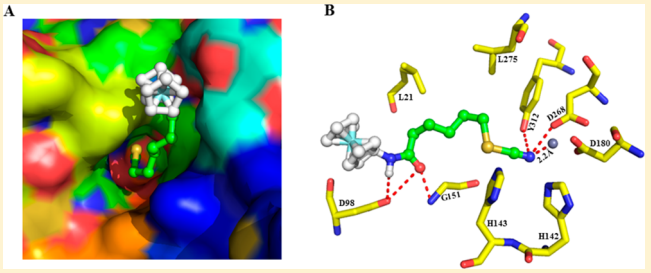

INTRODUCTION

In contrast to other subtypes of breast cancer,[1,2] triple-negative breast cancer (TNBC) usually occurs in young women and is very prone to exacerbation.[3] Because of the lack of expression of estrogen receptors (ERs) and progesterone receptors (PRs), as well as human epidermal growth factor receptor-2 (HER-2) in TNBC, traditional targeted therapies such as endocrine therapy and treatment with aromatase inhibitors are ineffective.[4] Therefore, much effort has been made to identify new prognostic markers or therapeutic targets to improve the treatment efficacy against TNBC.[5−7]

Previous studies have shown that the lack of ERα gene expression in TNBC is due to epigenetic changes, including increased deacetylation and methylation.[8−10] Accordingly, histone deacetylase (HDAC) inhibitors (HDACis) such as suberoylanilide hydroxamic acid (SAHA or vorinostat; Figure 1) and DNA methyltransferase inhibitors such as 5-aza-2′-deoxycytidine have been successfully used to reactivate the expression of ERα and simultaneously sensitize TNBC to treatment with antiestrogen drugs.[11,12] A combination of HDACis such as panobinostat or scriptaid with tamoxifen has been reported to enhance the therapeutic effects of tamoxifen through the activation of ERα gene (*ESR1*) expression.[13,14] Therefore, reactivation of the ERα expression by increasing histone acetylation can be used for the treatment of TNBC.

Currently, a large number of structurally diverse HDACis have been reported, and many of them are hydroxamic acid derivatives,[15] including the three U.S. Food and Drug Administration (FDA) approved HDACis SAHA,[16] belinostat (PXD101; Figure 1),[17] and panobinostat (LBH-589; Figure 1).[18] Although the hydroxamic acid group can interact with the Zn^{2+} ion in the active site of HDAC and is frequently employed as the zinc-binding group (ZBG), one of the major barriers for the development of hydroxamic acid derivatives as clinical drugs is their toxicity. They are prone to hydrolysis, resulting in the formation of potentially mutagenic hydroxylamine;[19] in addition, metabolic and pharmacokinetic problems also seriously hinder their clinical application.[20] Therefore, a number of new and nonhydroxamic acid derived inhibitors

Received: May 25, 2018

DOI: 10.1021/acs.organomet.8b00354
Organometallics XXXX, XXX, XXX−XXX

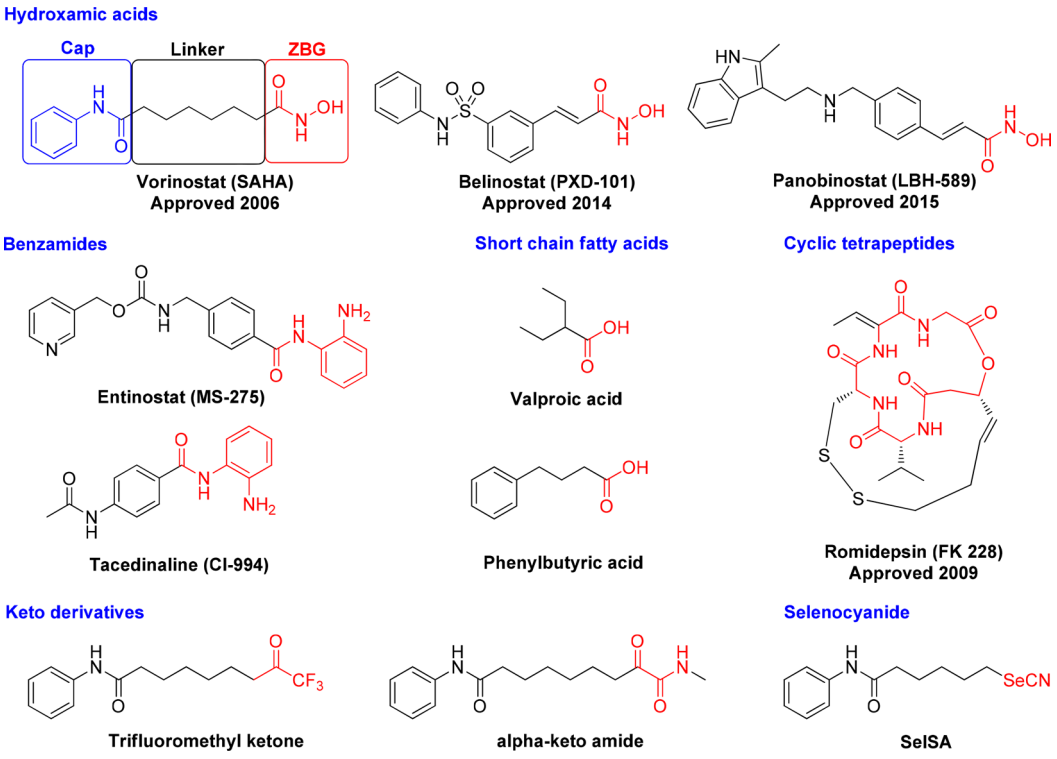

Figure 1. HDAC inhibitors and their pharmacophores.

Scheme 1. Synthesis of Ferrocenyl Derivatives 5 and 7

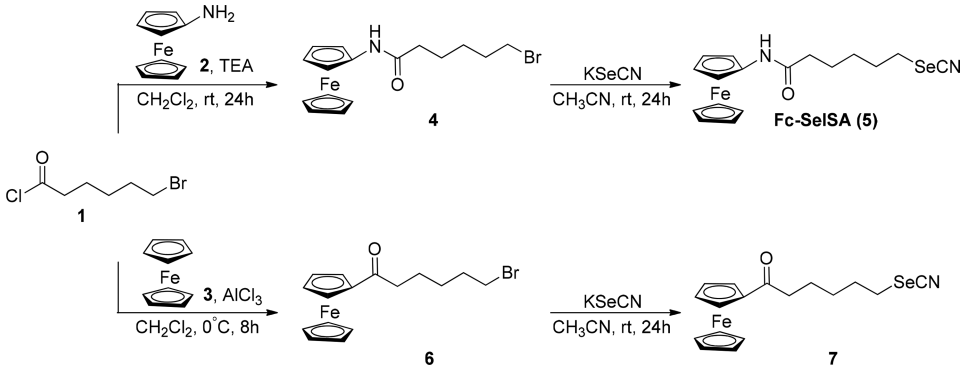

have been reported to date, including benzamides (entinostat (MS-275), tacedinaline (CI-994); Figure 1), short-chain fatty acids (valproic and phenylbutyric acids; Figure 1), cyclic tetrapeptides (romidepsin (FK-228); Figure 1), and keto derivatives (trifluoromethyl ketone and α-keto amide; Figure 1).[21−23] However, benzamides, short-chain fatty acids, cyclic tetrapeptides, and keto derivatives often have reduced potencies in comparison with those of hydroxamic acid derived inhibitors. Encouragingly, Desai et al.[24] have recently reported that a selenocyanide group containing analogue of SAHA (named SelSA; Figure 1) seemed to show a reasonable zinc-binding activity and exhibited a more than 20-fold greater potency against HDAC in comparison to that of SAHA. While it is structurally similar to SAHA, the phenyl capping unit of SelSA makes contacts with the pocket entrance in HDAC and, if replaced with other hydrophobic aromatic rings, can increase the HDAC inhibition activity, owing to the so-called "cap-linker-ZBG" pharmacophore of SAHA.

Previous studies from Jaouen's group[25−27] and our group[28] have demonstrated that organometallic ferrocene (Fc) derivatives can exhibit significant antiproliferative effects on TNBC cells and act as effective metallodrugs. In addition, incorporation of the Fc unit into ligands has a potential benefit of filling the active-site space, which is not possible with alicyclic or simple planar aromatic systems and can enhance the ligand-binding affinity.[29,30] In this study, we developed a metal cap based SelSA derivative and examined the effects of a nonplanar phenyl ring, the Fc unit, on HDAC inhibition and anticancer activity. Subsequently, reactivation of the ERα expression, due to anti-HDAC function, and anti-breast-cancer effects of the synthesized ferrocenyl analogues were further evaluated.

RESULTS AND DISCUSSION

Chemistry. The synthetic procedures for the ferrocenyl derivatives Fc-SelSA (**5**) and **7** were performed according to Scheme 1. Commercially available 6-bromohexanoyl chloride (**1**) was used as the starting material; it was treated with aminoferrocene (**2**) to obtain a key intermediate (**4**).

DOI: 10.1021/acs.organomet.8b00354
Organometallics XXXX, XXX, XXX−XXX

Meanwhile, **1** was allowed to react with Fc (**3**) in the presence of $AlCl_3$ to afford another intermediate (**6**). Subsequently, intermediates **4** and **6** were further treated with KSeCN in CH_3CN to produce the target selenocyanides Fc-SelSA (**5**) and **7**, respectively.

In Vitro Enzyme Inhibition. To determine whether the ferrocenyl moiety is a suitable surface-recognition cap group for a prototypical selenocyanide HDACi, we initially synthesized Fc-SelSA (**5**), in which the cap phenyl ring of SelSA was replaced with a ferrocenyl unit. Subsequently, HDAC inhibition activities of SelSA and the Fc-SelSA were tested in an in vitro fluorescence assay using a HeLa nuclear extract as the source of HDAC activity. Figure 2 shows that the

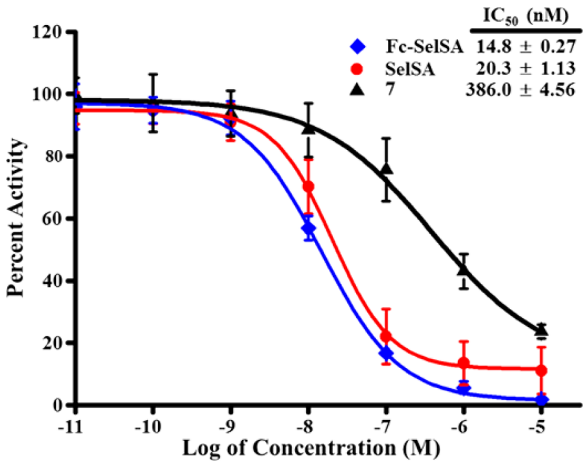

Figure 2. Inhibitory activities of Fc-SelSA, SelSA, and derivative **7** against HDAC using a HeLa nuclear extract.

inhibitory activity of Fc-SelSA (IC_{50} = 14.8 ± 0.07 nM) was significantly higher than that of the lead compound SelSA (IC_{50} = 20.3 ± 1.13 nM). This result indicated that the use of the nonplanar ferrocenyl moiety as a cap group was a successful strategy for the design of HDACis, which allowed an enhancement of the HDAC inhibition activity. Molecular docking simulations (see below) further demonstrated that the ferrocenyl of Fc-SelSA could be better accommodated in the active-site pocket of HDAC in comparison to the phenyl of SelSA, which allowed the amido group of Fc-SelSA to form hydrogen bonds with residues of the active pocket, which SelSA was not able to do. To evaluate the influence of the hydrogen-bond interactions, analogue **7**, in which the amido group of Fc-SelSA was replaced with a carbonyl group, was also tested in the HDAC inhibition assay; however, **7** displayed a 26-fold lower activity in comparison to that of Fc-SelSA. This result indicated that the hydrogen-bond interactions of the amido group were necessary for potent activity.

HDAC Docking Analysis. To understand how Fc-SelSA binds to HDAC, we performed a docking study with Fc-SelSA and HDAC (PDB: 1ZZ1) to examine the binding mode, and the results are shown in Figure 3. Similar to the case for traditional hydroxamic acid HDACis, such as SAHA, the two selenocyanide compounds SelSA and Fc-SelSA also adopted an optimal binding pose in the HDAC active-site pocket (Figure 3A–C), and the selenium atom of the selenocyanide group was able to coordinate perfectly with the catalytic zinc ion (Zn^{2+}–Se of SeCN: 2.5 Å for SelSA and 2.2 Å for Fc-SelSA). Additionally, the selenocyanide group of SelSA and Fc-SelSA is engaged in the key hydrogen-bond formation with Y312 (Figure 3E,F). This hydrogen bond is critical for stabilizing inhibitor chelation with the zinc ion in the catalytic domain. The hydroxamic acid group of the reference compound SAHA also formed a hydrogen bond with Y312 (Figure 3D). The selenocyanide group also formed another hydrogen bond, with D268 (Figure 3E,F), but SAHA did not form this hydrogen bond. This might explain why the selenocyanide compounds (SelSA and Fc-SelSA) had stronger HDAC inhibition activities in comparison to SAHA. More importantly, the ferrocenyl unit overlapped with the phenyl of SAHA, and the amido group of

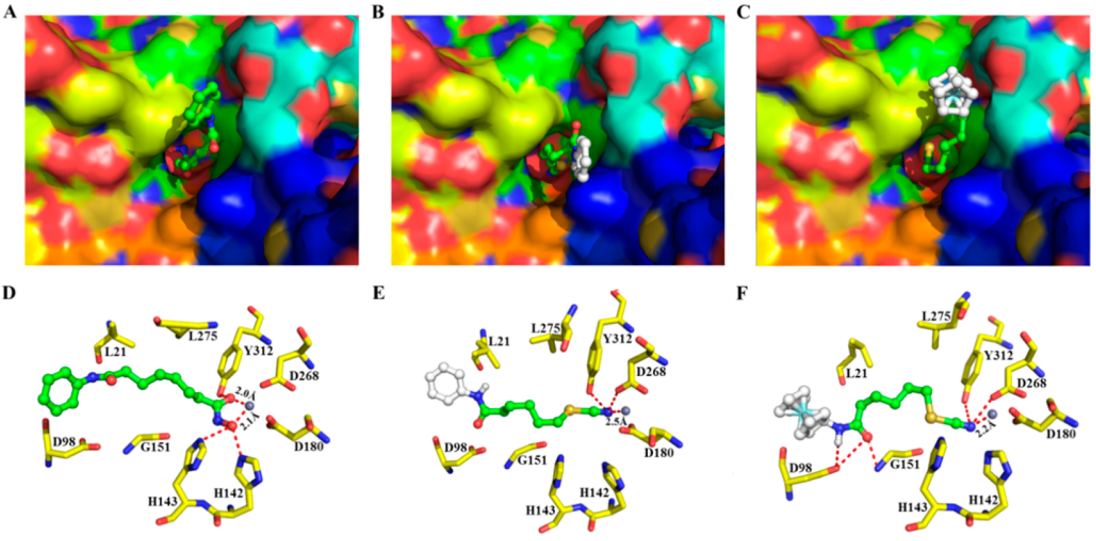

Figure 3. Docked complexes of SAHA, SelSA, and Fc-SelSA bound to HDAC. (A) Surface representation of the HDAC-SAHA complex. (B) Surface representation of the HDAC-SelSA complex. (C) Surface representation of the HDAC-Fc-SelSA complex. (D) Docking poses of SAHA in HDAC that can form hydrogen bonds with residues H142, H143, and Y312. (E) Docking poses of SelSA in HDAC that can form hydrogen bonds with residues D268 and Y312. (F) Docking poses of Fc-SelSA in HDAC that can form hydrogen bonds with residues D98, G151, D268, and Y312. The zinc ion is shown as a gray ball; interactions between the selenocyanide (SeCN) group and zinc are shown as red dashed lines. Distances are provided in Å.

DOI: 10.1021/acs.organomet.8b00354
Organometallics XXXX, XXX, XXX–XXX

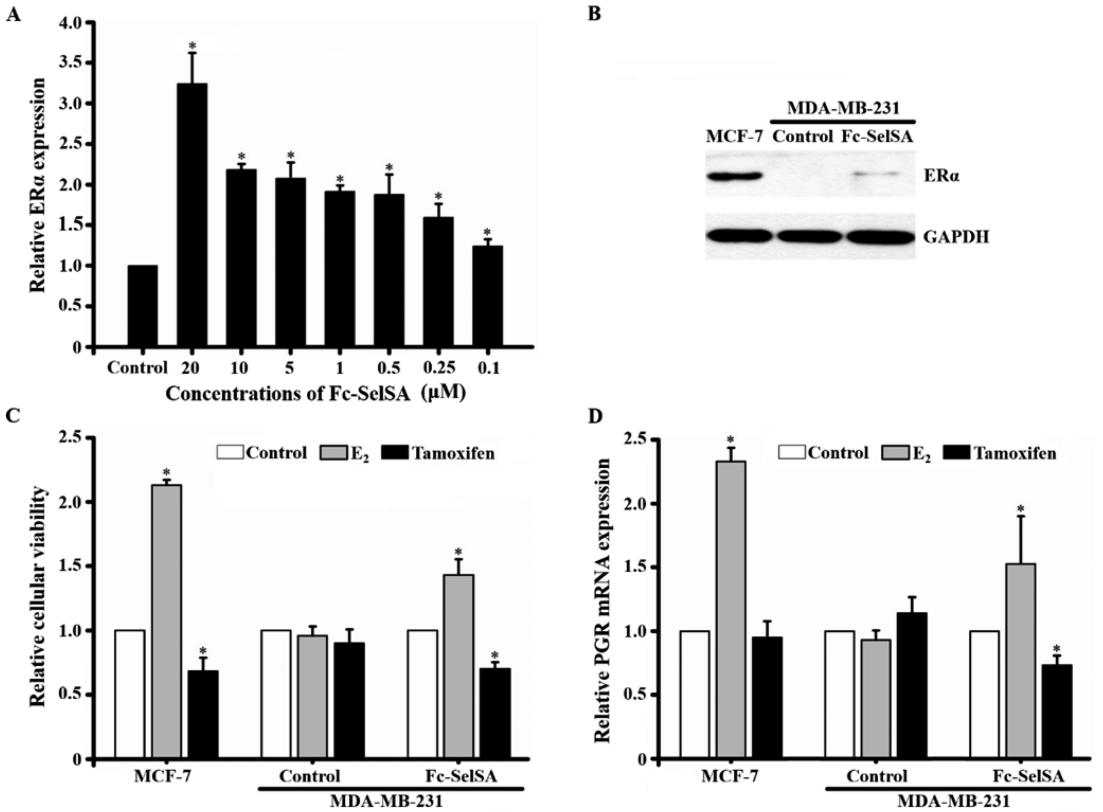

Figure 4. Fc-SelSA activation of the ERα expression and sensitization of MDA-MB-231 cells to E_2 and tamoxifen treatment. (A) *ESR1* mRNA expression induced by Fc-SelSA in MDA-MB-231 cells in a dose-dependent manner, as measured by qPCR. (B) ERα protein expression in MDA-MB-231 cells treated with Fc-SelSA. (C) Relative viability of MDA-MB-231 cells in response to E_2 and tamoxifen treatment, with or without Fc-SelSA. MCF-7 cells were used as a positive control. (D) Relative *PGR* mRNA expression in MDA-MB-231 cells in response to E_2 and tamoxifen treatment. MCF-7 cells were used as a positive control. Legend: (*) $P < 0.05$.

Fc-SelSA can form hydrogen bonds with the D98 and G151 residues (Figure 3F), whereas SAHA and SelSA did not have similar hydrogen-bonding interactions with D98 and G151. Thus, Fc-SelSA displayed the most potent anti-HDAC activity among these three HDACis.

Reactivation of ERα Expression. One efficient strategy for TNBC-targeted therapy is to change TNBC into ERα positive by reactivation of the *ESR1* gene expression. Previous studies have shown that HDACis can reactivate ERα expression in TNBC.[11,12] We therefore investigated the effects of Fc-SelSA on the expression of ERα mRNA and protein in MDA-MB-231 cells using qPCR and Western blot assays, respectively. As shown in Figure 4A, Fc-SelSA treatment resulted in a significantly increased expression of *ESR1* mRNA ($P < 0.05$) in comparison with the control. Importantly, expression of the ERα protein was also observed in MDA-MB-231 cells after treatment with Fc-SelSA (Figure 4B). We further examined whether this effect can render the TNBC responsive to the ER ligand estradiol (E_2) or the ER antagonist tamoxifen. The results indicated that ERα-positive MCF-7 cells showed good responses to both E_2 and tamoxifen, whereas the cell viability as well as the expression of the *PGR* gene, an ERα-responsive downstream gene, was unaffected by E_2 and tamoxifen in MDA-MB-231 cells without Fc-SelSA treatment (Figure 4C,D). In contrast, treatment with Fc-SelSA resulted in a significant change in the MDA-MB-231 cell viability and *PGR* expression, which was similar to those of MCF-7 cells in response to these two compounds (E_2 and tamoxifen). These results suggest that Fc-SelSA possesses the potential for therapeutic applications for TNBC through reactivation of the ERα expression and sensitization of cells to endocrine therapy.

Antiproliferative Activity of Fc-SelSA in Vitro. To investigate the cell-type selectivity and anticancer potency of Fc-SelSA, compounds Fc-SelSA and 7 were screened against the two breast cancer cell lines MCF-7 (hormone-dependent breast cancer) and MDA-MB-231 (TNBC) by the MTS assay using SelSA as a positive control. As expected, Fc-SelSA was much more potent than SelSA against both MCF-7 and MDA-MB-231 cells (Table 1). In particular, Fc-SelSA (CC_{50} = 0.17 ± 0.07 μM; the dose–response curves are shown in Figure S1) inhibited the MDA-MB-231 cell growth 4-fold more potently than SelSA and showed a 7-fold greater selectivity for MDA-MB-231 cells over MCF-7 cells. However, the replacement of the amido group of Fc-SelSA with a carbonyl group (compound 7) resulted in at least a 4-fold decrease of its antiproliferative activity against both MCF-7 and MDA-MB-

Table 1. Antiproliferative Activities of SelSA and Ferrocenyl Derivatives

	CC_{50} (μM)[a]			
compound	MCF-7	MDA-MB-231	MCF-10A	Vero
SelSA	1.36 ± 0.11	0.64 ± 0.06	>100[b]	>100
Fc-SelSA	1.18 ± 0.34	0.17 ± 0.03	>100	>100
7	5.46 ± 0.49	2.04 ± 0.27	>100	>100

[a]CC_{50} values are the mean ± standard deviation of at least three independent experiments. [b]The highest concentration tested.

DOI: 10.1021/acs.organomet.8b00354
Organometallics XXXX, XXX, XXX−XXX

Table 2. Acute Toxicity of Fc-SelSA in Healthy Mice

		mortality						
dose (mg/kg)	no. of mice	1 h	5 h	4 days	5–21 days	total mortality	survival (%) on day 21	LD_{50}[a] (mg/kg)
895	8	1	2	5	0	8	0	605.6
716	8	0	1	5	0	6	25.0	
573	8	0	0	3	0	3	62.5	
458.4	8	0	0	1	0	1	87.5	
366.7	8	0	0	0	0	0	100	

[a]The 95% confidence limits: 541.14–677.94 mg/kg.

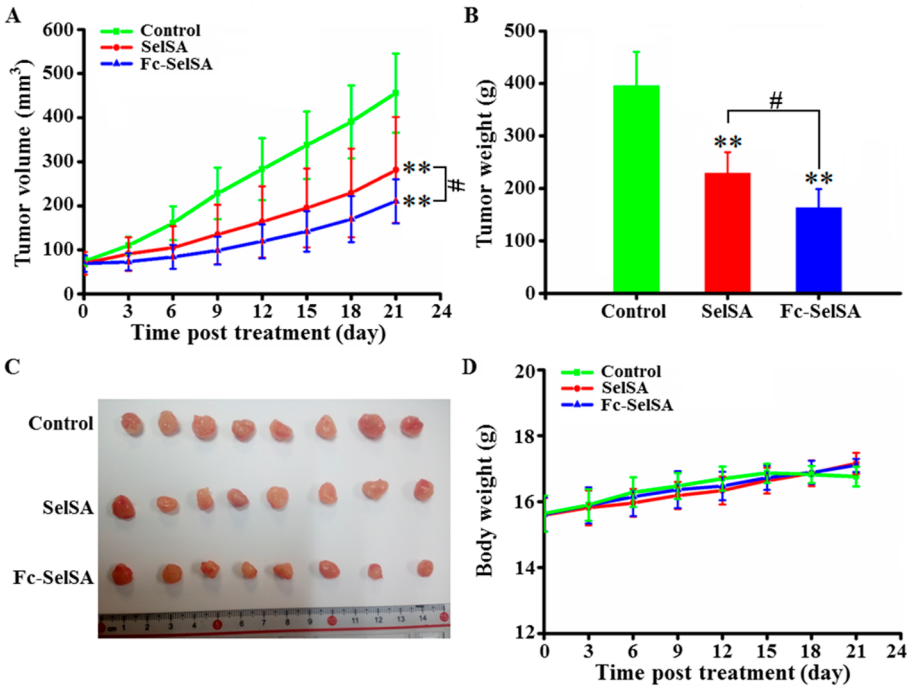

Figure 5. Antitumor effects of Fc-SelSA and SelSA on MDA-MB-231 breast tumor xenograft mouse model. (A) Average tumor volumes in xenograft mice after different treatments. (B) Average tumor weights in xenograft mice after different treatments. (C) Tumors dissected at the end of experiment. (D) Average body weight changes in xenograft mice over a period of 21 days with different treatments. Legend: (**) $P < 0.01$ vs the control; (#) $P < 0.05$, the Fc-SelSA treatment group vs the SelSA group.

231 cells and in a 3-fold weaker cell-type selectivity, which agrees with the poor HDAC inhibition profile of **7**. These above results indicate that the antiproliferative activity of the ferrocenyl compounds Fc-SelSA and **7** against MDA-MB-231 cells is related to the inhibition of HDAC, and the introduction of the ferrocenyl group can enhance potency against MDA-MB-231 cells.

Since the cytotoxicity is important for an anticancer compound, we further tested Fc-SelSA, **7**, and SelSA against the noncancer cells MCF-10A (human normal breast epithelial cells) and Vero (healthy kidney epithelial cells). Our study has indicated that the FDA-approved SAHA showed considerable toxicity to the healthy cells (Vero), while our selenocyanide compounds (Fc-SelSA, **7**, and SelSA) were nontoxic to healthy cells (MCF-10A and Vero).

Safety Profile of Fc-SelSA in Healthy Mice. Since Fc-SelSA showed significant antiproliferative effects in vitro, its therapeutic efficacy was studied in vivo. First, an acute toxicity test was performed to evaluate the safety of Fc-SelSA in healthy mice. Adult BALB/c mice ($n = 8$) were treated with Fc-SelSA at 895, 716, 573, 458.4, and 366.7 mg/kg by oral gavage, and the survival of these mice was continuously monitored for 21 days after treatment. The oral treatment with 366.7 mg/kg Fc-SelSA did not cause any death, whereas all the mice were killed at a dose of 895 mg/kg. The survival rates were 87.5%, 62.5%, and 25% at doses of 458.4, 573, and 716 mg/kg, respectively (Table 2). On the basis of these data, the median lethal dose (LD_{50}) value of Fc-SelSA was calculated to be 605.6 mg/kg.

In Vivo Anticancer Activity. To evaluate the in vivo anticancer activity of Fc-SelSA, it was orally administered at 20 mg/kg daily for 21 days, and SelSA was administered at the same dose as a positive control. As shown in Figure 5, treatment with SelSA and Fc-SelSA significantly reduced the tumor volumes in the MDA-MB-231 tumor-bearing mouse model ($P < 0.01$ vs control; Figure 5A); the tumor volume in the Fc-SelSA-treated mice was smaller than that in the mice administered SelSA ($P < 0.05$; Figure 5A). Moreover, Fc-SelSA treatment significantly reduced the weight of MDA-MB-231 tumor xenografts by 58.6% ($P < 0.01$ vs control), which was superior to the effect observed in the SelSA group (41.9% reduction vs control; $P < 0.01$ vs control; Figure 5B,C). Additionally, the body weights in the tumor-bearing mice treated with Fc-SelSA and SelSA were not significantly affected, and no adverse side effects were observed during the treatment period (Figure 5D). Taken together, these

DOI: 10.1021/acs.organomet.8b00354
Organometallics XXXX, XXX, XXX–XXX

results highlighted the superior anti-TNBC effects of Fc-SelSA, in comparison with those of SelSA, with no adverse side effects. Thus, Fc-SelSA may be used as a novel and potent HDACi for TNBC therapy.

CONCLUSIONS

Due to the lack of targeted therapies, it is difficult to effectively treat TNBC. HDAC have emerged as effective targets for the development of anti-TNBC agents because of their association with ERα expression-reactivating effects. In the present study, we designed, synthesized, and evaluated a novel metallic HDACi with a Fc cap (Fc-SelSA) for the treatment of TNBC. We found that the replacement of the phenyl ring of SelSA with a nonplanar bioisostere ferrocenyl group resulted in a more potent anti-HDAC activity of the compound. Subsequent molecular docking analysis showed that the ferrocenyl group overlaps with the phenyl ring, allowing the amido group of Fc-SelSA to form hydrogen-bonding interactions with residues D98 and G151, which SAHA and SelSA were not able to do. These results indicated that using a three-dimensional aryl group as a cap is an effective strategy for the design of HDACis. Moreover, Fc-SelSA treatment can induce the ERα expression in TNBC and sensitize MDA-MB-231 cells to conventional endocrine therapy by reactivating ERα. Furthermore, Fc-SelSA was selectively more potent against MDA-MB-231 cells in comparison to MCF-7 cells with no toxicity against normal cells in the in vitro antiproliferation test. In addition, Fc-SelSA showed a relatively low acute toxicity in mice, and treatment with Fc-SelSA significantly inhibited the growth of TNBC in a xenograft mouse model in comparison to SelSA ($P < 0.05$). Given its high HDAC-binding affinity and potent therapeutic effect, Fc-SelSA can therefore serve as a promising targeting ligand to study HDAC-related epigenetic changes during tumorigenesis and as an anti-TNBC therapeutic agent.

EXPERIMENTAL SECTION

General Reagents and Methods. All chemical reagents and solvents were purchased from Aldrich, Acros, Aladdin Reagents, and Alfa Aesar. Dichloromethane and acetonitrile were distilled from anhydrous CaH_2. Unless otherwise noted, all reactions were conducted under an inert (Ar) atmosphere. The reaction progress was monitored by analytical thin-layer chromatography under UV light (254 nm).

^{1}H NMR and ^{13}C NMR spectra were measured on a Bruker Biospin AV400 instrument (at 400 and 100 MHz, respectively). Chemical shifts are reported in ppm and are referenced to either tetramethylsilane or the solvent. The purity of all compounds (>95%) for biological testing was confirmed by high-performance liquid chromatography.

Synthesis of 7-Bromoheptanoic Acid Ferrocenylamide (4). To a solution of aminoferrocene were added **2** (0.904 g, 4.5 mmol), in dry CH_2Cl_2 (30 mL), cooled to 0 °C, triethylamine (0.688 g, 6.8 mmol), and 6-bromohexanoyl chloride (**1**; 1.153 g, 5.4 mmol) under an Ar atmosphere. The reaction solution was warmed to room temperature and then stirred for 24 h. Subsequently, the reaction mixture was poured into water and extracted with CH_2Cl_2 (3 × 30 mL). The extracts were dried (anhydrous Na_2SO_4) and evaporated. The crude product was purified by silica gel column chromatography (petroleum ether/ethyl acetate (EtOAc), 9/1) to yield bromo amide **4** as a red oil (1.509 g, 88.7% yield). ^{1}H NMR (400 MHz, CD_3OD): δ 4.61 (s, 2H), 4.15 (s, 5H), 4.00 (s, 2H), 3.60 (t, J = 6.0 Hz, 2H), 2.28 (t, J = 7.2 Hz, 2H), 1.81−1.85 (m, 2H), 1.69−1.73 (m, 2H), 1.53−1.57 (m, 2H). ^{13}C NMR (100 MHz, CD_3OD): δ 172.85, 94.44, 68.75, 64.06, 61.14, 44.26, 36.04, 32.11, 26.16, 24.95.

Synthesis of 5-Ferrocenylcarbamoylpentyl Selenocyanide (Fc-SelSA, 5). To a solution of bromo amide **4** (1.475 g, 3.9 mmol), in dry acetonitrile (25 mL), was added KSeCN (0.682 g, 4.7 mmol). The reaction solution was stirred at room temperature for 24 h under an Ar atmosphere. The solvent was removed by rotary evaporation to yield the crude product, which was purified by silica gel column chromatography (petroleum ether/EtOAc, 3/2). The Fc-SelSA product was isolated (1.232 g, 78.3% yield) as a red solid. ^{1}H NMR (400 MHz, CD_3OD): δ 4.62 (s, 2H), 4.15 (s, 5H), 4.00 (s, 2H), 3.59 (t, J = 7.2 Hz, 2H), 2.28 (t, J = 6.8 Hz, 2H), 1.78−1.82 (m, 2H), 1.68−1.72 (m, 2H), 1.51−1.56 (m, 2H). ^{13}C NMR (100 MHz, CD_3OD): δ 172.78, 102.79, 94.37, 68.75, 64.07, 61.18, 35.92, 30.60, 29.09, 28.21, 24.86. HRMS (ESI): calcd for $C_{17}H_{21}{}^{54}FeN_2OSe$ $[M + H]^+$, 402.1664; found, 402.1669.

Synthesis of 6-Bromo-1-Ferrocenylhexan-1-one (6). To a solution of 6-bromohexanoyl chloride (**1**; 4.932 g, 23.1 mmol) and $AlCl_3$ (9.241 g, 69.3 mmol) in dry CH_2Cl_2 (60 mL) at 0 °C was added a solution of Fc (**3**; 2.141 g, 11.5 mmol) in dry CH_2Cl_2 (30 mL) dropwise over 20 min under an Ar atmosphere. After the solution was stirred for 12 h at room temperature, saturated $NaHCO_3$ (50 mL) was added, and the mixture was extracted with CH_2Cl_2 (3 × 60 mL). The extracts were dried (anhydrous Na_2SO_4) and concentrated. The crude product was purified by silica gel column chromatography (petroleum ether/EtOAc, 9/1) to yield the bromo intermediate **6** as a red solid (1.282 g, 30.7% yield). ^{1}H NMR (400 MHz, $CDCl_3$): δ 4.78 (s, 2H), 4.50 (s, 2H), 4.19 (s, 5H), 3.44 (t, J = 6.4 Hz, 2H), 2.72 (t, J = 7.2 Hz, 2H), 1.89−1.96 (m, 2H), 1.70−1.77 (m, 2H), 1.52−1.57 (m, 2H). ^{13}C NMR (100 MHz, $CDCl_3$): δ 204.21, 79.03, 72.23, 69.78, 69.32, 39.40, 33.78, 32.69, 28.08, 23.58.

Synthesis of 5-Ferrocenyl Carbonylpentyl Selenocyanide (7). The process was performed as for the preparation of Fc-SelSA using the bromo intermediate **6**, instead of **4**, to afford selenocyanide **7**. A red solid was obtained in 82.5% yield. ^{1}H NMR (400 MHz, $CDCl_3$): δ 4.78 (s, 2H), 4.50 (s, 2H), 4.19 (s, 5H), 3.10 (t, J = 7.2 Hz, 2H), 2.74 (t, J = 7.2 Hz, 2H), 1.93−2.01 (m, 2H), 1.72−1.79 (m, 2H), 1.50−1.58 (m, 2H). ^{13}C NMR (100 MHz, $CDCl_3$): δ 203.95, 101.58, 78.96, 72.26, 69.78, 69.29, 39.14, 30.74, 29.38, 28.81, 23.47. HRMS (ESI): calcd for $C_{17}H_{20}{}^{54}FeNOSe$ $[M + H]^+$, 387.1518; found, 387.1522.

Cell Lines. Breast cancer MCF-7 and MDA-MB-231 cells were purchased from the American Type Culture Collection (ATCC). Human normal breast epithelial cells (MCF-10A) and healthy kidney epithelial cells (VERO) were purchased from the cell bank of the Chinese Academy of Sciences (Shanghai, People's Republic of China). The cells were cultured in Dulbecco Minimum Essential Medium (DMEM, Hyclone, Thermo Scientific, Waltham, USA) containing 10% (v/v) fetal bovine serum (FBS, Hyclone, Thermo Scientific) and 1% (v/v) penicillin/streptomycin. Cells were maintained at 37 °C 5% in a CO_2 incubator.

HDAC Inhibition Assay. The HDAC inhibition activity was measured using an HDAC assay kit (BPS Bioscience) according to a previously described method.[28,31] Half-maximum inhibitory concentration (IC_{50}) values were calculated from dose−response curves using Origin software (OriginLab, Inc.).

Western Blot Analysis. MDA-MB-231 cells were treated with Fc-SelSA for 48 h and then lysed in RIPA buffer. Total protein was separated by electrophoresis in Tris-glycine gradient gels and then analyzed by Western blotting. The primary antibody was anti-ERα (Pierce; 1/1000 dilution), and the secondary antibody was horseradish peroxidase conjugated antigoat IgG or an antirabbit antibody (Pierce; 1/10000 dilution).

Molecular Modeling. The crystal structure of HDAC (PDB: 1ZZ1) was obtained from the Protein Data Bank,[32] and all water molecules were removed. Crystallographic coordinates of SelSA and Fc-SelSA were prepared using BioChem Office software. Preparation of the ligands and protein was performed with AutoDockTools, and molecular docking experiments were performed using AutoDock software (version 4.2). The figures were prepared using PyMOL (Erwin Schrödinger).

DOI: 10.1021/acs.organomet.8b00354
Organometallics XXXX, XXX, XXX−XXX

ERα Expression Reactivation Assays. To evaluate the effects of Fc-SelSA on ERα expression, MDA-MB-231 cells were treated with Fc-SelSA for 3 days, and then ERα mRNA and protein expression was examined using quantitative real-time PCR (qPCR) and Western blotting assays, as previously described.[19] The PCR primers used were the ERα ligand-binding domain forward (5′-ATAGGATCCATC-AAACGCTCTAAGAAG-3′) and reverse (5′-ATACTCGAGGC-TAGTGGGCGCATGTAG-3′) primers.[9]

To investigate whether Fc-SelSA can enable TNBC cells to respond to estradiol (E_2) and tamoxifen by reactivating the ERα expression, Fc-SelSA-pretreated MDA-MB-231 cells were treated with 10 nM E_2 or 1 μM tamoxifen for 2 days, and then cell viability was evaluated using a standard MTS assay (Biovision, Inc.). The expression of the PR-encoding gene (*PGR*), an ERα target gene, was also detected using real-time PCR with the following oligonucleotide primers: forward (5′-AACTGCCCAGCATGTC-GCCT-3′) and reverse (5′-GGAACGCCCACTGGCTGTGG-3′).[9]

Cell Proliferation Assay. The antiproliferative effects of SelSA and Fc-SelSA were evaluated using the MTS assay according to a previously described method.[28,32] CC_{50} (50% cytotoxic concentration) values were calculated from dose−response curves using Origin software (OriginLab, Inc.).

Establishment of a Tumor-Bearing Mouse Model. Female BALB/c mice (6 weeks old, 15−18 g) were purchased from Beijing Vital River Laboratory Animal Technology Co., Ltd. All animal study procedures were approved by the Institutional Animal Care and Use Committee at Peking University (Permit No. 2011-0039). MCF-7 and MDA-MB-231 cells were transplanted subcutaneously in the axillary region of the mice.

Statistics. Data are shown as the means ± SD from three independent experiments. One-way ANOVA with a Tukey test was performed to compare differences between groups, and a two-tailed Student's *t* test was performed to compare two groups. LegendL (*) $P < 0.05$ was considered statistically significant.

■ ASSOCIATED CONTENT

Supporting Information

The Supporting Information is available free of charge on the ACS Publications website at DOI: 10.1021/acs.organomet.8b00354.

Dose−response curves and ^{1}H NMR and ^{13}C NMR spectral information for compounds **5** and **7** (PDF)

■ AUTHOR INFORMATION

Corresponding Authors

*Z.C.: e-mail, zcheng@stanford.edu; tel, 650-723-7866; fax, 650-736-7925.

*J.T.: e-mail, jie.tian@ia.ac.cn, tian@ieee.org; tel, 8610 62527995; fax, 86 10 62527995; web, http://www.3dmed.net.

ORCID

Zhen Cheng: 0000-0001-8177-9463

Jie Tian: 0000-0002-9523-2271

Author Contributions

#C.T. and Y.D. contributed equally to this work.

Notes

The authors declare no competing financial interest.

■ ACKNOWLEDGMENTS

This paper was supported by the Ministry of Science and Technology of China under Grant Nos. 2017YFA0205200 and 2016YFC0102000, the National Natural Science Foundation of China under Grant Nos. 81470083, 81527805, 61231004, 81601548, 81701771, and 81772011, the International Innovation Team of CAS under Grant No. 20140491524, Beijing Municipal Science & Technology Commission No. Z161100002616022, the Fundamental Research Funds for the Central universities (JB161204, JBG161201, XJS16011), China Postdoctoral Science Foundation funded project (2017M613084), and Shaanxi Postdoctoral Science Foundation funded project (2017BSHEDZZ91).

■ REFERENCES

(1) Dent, R.; Trudeau, M.; Pritchard, K. I.; Hanna, W. M.; Kahn, H. K.; Sawka, C. A.; Lickley, L. A.; Rawlinson, E.; Sun, P.; Narod, S. A. Triple-negative breast cancer: clinical features and patterns of recurrence. *Clin. Cancer Res.* **2007**, *13* (15), 4429−4434.

(2) Carey, L.; Winer, E.; Viale, G.; Cameron, D.; Gianni, L. Triple-negative breast cancer: disease entity or title of convenience? *Nat. Rev. Clin. Oncol.* **2010**, *7* (12), 683−692.

(3) Narod, S. A. Breast cancer in young women. *Nat. Rev. Clin. Oncol.* **2012**, *9* (8), 460−470.

(4) Papa, A.; Caruso, D.; Tomao, S.; Rossi, L.; Zaccarelli, E.; Tomao, F. Triple-negative breast cancer: investigating potential molecular therapeutic target. *Expert Opin. Ther. Targets* **2015**, *19* (1), 55−75.

(5) Barbie, T. U.; Alexe, G.; Aref, A. R.; Li, S.; Zhu, Z.; Zhang, X.; Imamura, Y.; Thai, T. C.; Huang, Y.; Bowden, M.; Herndon, J.; Cohoon, T. J.; Fleming, T.; Tamayo, P.; Mesirov, J. P.; Ogino, S.; Wong, K. K.; Ellis, M. J.; Hahn, W. C.; Barbie, D. A.; Gillanders, W. E. Targeting an IKBKE cytokine network impairs triple-negative breast cancer growth. *J. Clin. Invest.* **2014**, *124* (12), 5411−5423.

(6) Bianchini, G.; Balko, J. M.; Mayer, I. A.; Sanders, M. E.; Gianni, L. Triple-negative breast cancer: challenges and opportunities of a heterogeneous disease. *Nat. Rev. Clin. Oncol.* **2016**, *13* (11), 674−690.

(7) Fusella, F.; Seclì, L.; Busso, E.; Krepelova, A.; Moiso, E.; Rocca, S.; Conti, L.; Annaratone, L.; Rubinetto, C.; Mello-Grand, M.; Singh, V.; Chiorino, G.; Silengo, L.; Altruda, F.; Turco, E.; Morotti, A.; Oliviero, S.; Castellano, I.; Cavallo, F.; Provero, P.; Tarone, G.; Brancaccio, M. The IKK/NF-κB signaling pathway requires Morgana to drive breast cancer metastasis. *Nat. Commun.* **2017**, *8* (1), 1636.

(8) Zhou, Q.; Atadja, P.; Davidson, N. E. Histone deacetylase inhibitor LBH589 reactivates silenced estrogen receptor alpha (ER) gene expression without loss of DNA hypermethylation. *Cancer Biol. Ther.* **2007**, *6* (1), 64−69.

(9) Li, Y.; Yuan, Y. Y.; Meeran, S. M.; Tollefsbol, T. O. Synergistic epigenetic reactivation of estrogen receptor-α (ERα) by combined green tea polyphenol and histone deacetylase inhibitor in ERα-negative breast cancer cells. *Mol. Cancer* **2010**, *9*, 274−285.

(10) Sabnis, G. J.; Goloubeva, O.; Chumsri, S.; Nguyen, N.; Sukumar, S.; Brodie, A. M. Functional activation of the estrogen receptor-α and aromatase by the HDAC inhibitor entinostat sensitizes ER-negative tumors to letrozole. *Cancer Res.* **2011**, *71* (5), 1893−1903.

(11) Yang, X.; Phillips, D. L.; Ferguson, A. T.; Nelson, W. G.; Herman, J. G.; Davidson, N. E. Synergistic activation of functional estrogen receptor (ER)-α by DNA methyltransferase and histone deacetylase inhibition in human ER-α-negative breast cancer cells. *Cancer Res.* **2001**, *61* (19), 7025−7029.

(12) Khan, S. I.; Aumsuwan, P.; Khan, I. A.; Walker, L. A.; Dasmahapatra, A. K. Epigenetic events associated with breast cancer and their prevention by dietary components targeting the epigenome. *Chem. Res. Toxicol.* **2012**, *25* (1), 61−73.

(13) Sharma, D.; Saxena, N. K.; Davidson, N. E.; Vertino, P. M. Restoration of tamoxifen sensitivity in estrogen receptor-negative breast cancer cells: tamoxifen-bound reactivated ER recruits distinctive corepressor complexes. *Cancer Res.* **2006**, *66* (12), 6370−6378.

(14) Giacinti, L.; Giacinti, C.; Gabellini, C.; Rizzuto, E.; Lopez, M.; Giordano, A. Scriptaid effects on breast cancer cell lines. *J. Cell. Physiol.* **2012**, *227* (10), 3426−3433.

(15) Paris, M.; Porcelloni, M.; Binaschi, M.; Fattori, D. Histone deacetylase inhibitors: from bench to clinic. *J. Med. Chem.* **2008**, *51* (6), 1505−1529.

DOI: 10.1021/acs.organomet.8b00354
Organometallics XXXX, XXX, XXX−XXX

(16) Duvic, M.; Vu, J. Vorinostat: a new oral histone deacetylase inhibitor approved for cutaneous T-cell lymphoma. *Expert Opin. Invest. Drugs* **2007**, *16* (7), 1111−1120.
(17) Garnock-Jones, K. P. Panobinostat: first global approval. *Drugs* **2015**, *75* (6), 695−704.
(18) Poole, R. M. Belinostat: first global approval. *Drugs* **2014**, *74* (13), 1543−1554.
(19) Sanderson, L.; Taylor, G. W.; Aboagye, E. O.; Alao, J. P.; Latigo, J. R.; Coombes, R. C.; Vigushin, D. M. Plasma pharmacokinetics and metabolism of the histone deacetylase inhibitor trichostatin a after intraperitoneal administration to mice. *Drug Metab. Dispos.* **2004**, *32* (10), 1132−1138.
(20) Mulder, G. J.; Meerman, J. H. Sulfation and glucuronidation as competing pathways in the metabolism of hydroxamic acids: the role of N,O-sulfonation in chemical carcinogenesis of aromatic amines. *Environ. Health Perspect.* **1983**, *49* (4), 27−32.
(21) Bertrand, P. Inside HDAC with HDAC inhibitors. *Eur. J. Med. Chem.* **2010**, *45*, 2095−2116.
(22) Thaler, F.; Mercurio, C. Towards selective inhibition of histone deacetylase isoforms: what has been achieved, where we are and what will be next. *ChemMedChem* **2014**, *9* (3), 523−526.
(23) Roche, J.; Bertrand, P. Inside HDACs with more selective HDAC inhibitors. *Eur. J. Med. Chem.* **2016**, *121*, 451−483.
(24) Desai, D.; Salli, U.; Vrana, K. E.; Amin, S. SelSA, selenium analogs of SAHA as potent histone deacetylase inhibitors. *Bioorg. Med. Chem. Lett.* **2010**, *20* (6), 2044−2047.
(25) Plazuk, D.; Vessières, A.; Hillard, E. A.; Buriez, O.; Labbé, E.; Pigeon, P.; Plamont, M. A.; Amatore, C.; Zakrzewski, J.; Jaouen, G. A [3]ferrocenophane polyphenol showing a remarkable antiproliferative activity on breast and prostate cancer cell lines. *J. Med. Chem.* **2009**, *52* (15), 4964−4967.
(26) Cázares Marinero, J. d. J.; Lapierre, M.; Cavaillès, V.; Saint-Fort, R.; Vessières, A.; Top, S.; Jaouen, G. Efficient new constructs against triple negative breast cancer cells: synthesis and preliminary biological study of ferrocifen-SAHA hybrids and related species. *Dalton Trans.* **2013**, *42* (43), 15489−15501.
(27) Cázares-Marinero, J. d. J.; Top, S.; Vessières, A.; Jaouen, G. Synthesis and antiproliferative activity of hydroxyferrocifen hybrids against triple-negative breast cancer cells. *Dalton Trans.* **2014**, *43* (2), 817−830.
(28) Li, C. H.; Tang, C.; Hu, Z. Y.; Li, C. L.; Zhang, S. L.; Dong, C.; Zhou, H. B.; Huang, J. Synthesis and structure-activity relationships of novel hybrid ferrocenyl compounds based on a bicyclic core skeleton for breast cancer therapy. *Bioorg. Med. Chem.* **2016**, *24* (13), 3062−3074.
(29) Meggers, E. Targeting proteins with metal complexes. *Chem. Commun.* **2009**, *7* (9), 1001−1010.
(30) Spencer, J.; Amin, J.; Wang, M.; Packham, G.; Alwi, S. S.; Tizzard, G. J.; Coles, S. J.; Paranal, R. M.; Bradner, J. E.; Heightman, T. D. Synthesis and biological evaluation of JAHAs: ferrocene-based histone deacetylase inhibitors. *ACS Med. Chem. Lett.* **2011**, *2* (5), 358−362.
(31) Tang, C.; Li, C. H.; Zhang, S. L.; Hu, Z.; Wu, J.; Dong, C.; Huang, J.; Zhou, H. B. Novel bioactive hybrid compound dual targeting estrogen receptor and histone deacetylase for the treatment of breast cancer. *J. Med. Chem.* **2015**, *58* (11), 4550−4572.
(32) Gryder, B. E.; Rood, M. K.; Johnson, K. A.; Patil, V.; Raftery, E. D.; Yao, L. P.; Rice, M.; Azizi, B.; Doyle, D. F.; Oyelere, A. K. Histone deacetylase inhibitors equipped with estrogen receptor modulation activity. *J. Med. Chem.* **2013**, *56* (14), 5782−5796.

DOI: 10.1021/acs.organomet.8b00354
Organometallics XXXX, XXX, XXX−XXX